

# Magnetically Tunable Superconducting Microstrip Resonators Using Yttrium Iron Garnet Single Crystals

Makoto TSUTSUMI and Takeshi FUKUSAKO  
Kyoto Institute of Technology, Department of Electronics & Information Science  
Matsugasaki, Sakyo-ku, Kyoto 606, Japan

## ABSTRACT

A magnetically tunable microstrip superconducting resonator using an yttrium iron garnet (YIG) single crystal was demonstrated experimentally. Tunability of 200MHz at a center frequency of 5.3GHz was observed, and a quality factor of 965 with minimum insertion loss of 19.5dB was measured for a half-wavelength microstrip line consisting of a YIG-YBCO-MgO composite structure. The dispersion relation of the resonator was analyzed using the spectral domain method and discussed with experimental results on the mixed states of TEM and magnetostatic wave modes.

## I. INTRODUCTION

Applications of high-temperature superconductors to microwave devices have been extensively studied by many workers to obtain ultra low-loss, high-performance circuits and devices. Superconducting resonator structures of interest are microstrip line resonators fabricated on dielectric MgO substrates and dielectric resonators with superconducting walls. Recently, little effort has been devoted to ferrite-superconductor composite devices such as circulators and phase shifters without significant conductor losses[1][2] or to magnetically tunable filters using the vortex effect under weak magnetic fields[3].

The authors have studied, for the first time, a magnetically tunable superconducting microstrip line filter using Yttrium Iron Garnet (YIG) film grown epitaxially on a Gadolinium Gallium Garnet (GGG) substrate, and discussed the magnetic loss of the YIG film on the GGG substrate which significantly reduces the quality factor of the filter[4].

This paper investigates magnetically tunable superconducting half-wavelength microstrip line resonators using YBCO and YIG single crystal, and discusses the magnetically tunable characteristics of the resonators in experimental results with the calculated dispersion relation.

## II. EXPERIMENT

Figure 1 shows a superconducting microstrip line resonator composed of sandwiched structures of MgO-YBCO ( $YBa_2Cu_3O_7$ ) and YIG single crystal. The YIG single crystal was arranged on the YBCO strip to obtain strong interaction of rf fields with the superconductor. A half wavelength microstrip single resonator on  $17\text{mm} \times 10\text{mm}$  MgO substrates was designed with a  $50\text{ Ohm}$  characteristic impedance,  $10\text{mm}$  length, and  $0.5\text{mm}$  width. It was coupled with input and output lines with  $s=0.3\text{mm}$  and  $0.5\text{mm}$  capacitive gaps. The YBCO grown by laser deposition is  $0.6\mu\text{m}$  thick and has a  $T_c$  of  $86\text{K}$ .

The YIG single crystal was used to achieve magnetically tunable resonator characteristics to change susceptibility using an applied dc magnetic field, and to eliminate the effect on the lossy GGG substrate, which reduces the quality factor[4].

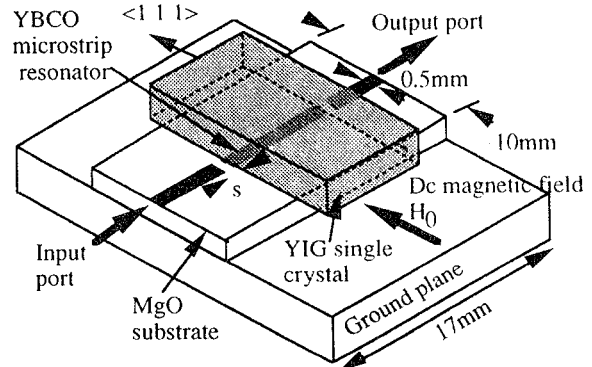


Figure 1: Magnetically tunable superconducting half wavelength microstrip line resonator.

The YIG is a  $10\text{mm} \times 10\text{mm}$ ,  $1\text{mm}$  thick in  $(2\ 1\ 1)$  plane with a magnetic line width of  $\Delta H=1\text{Oe}$  at room temperature and at X band. The YIG is the same length as the half wavelength of the resonator.

The resonator test structure of Fig. 1 was shielded by aluminium foil to suppress the radiation loss arising from the discontinuities between the input-output terminals and the stripline. The dc magnetic field was applied in the transverse direction to the wave propagation as shown in Fig.s 1 and 2 by a pair of Helmholtz coils of 300 turns each. Such a magnetic field direction has less demagnetizing effect and strong interaction between the superconductor and surface wave mode. The magnetic field intensity at the center of the coil was about 200 Gauss per ampere. The test set up was then immersed into liquid nitrogen together

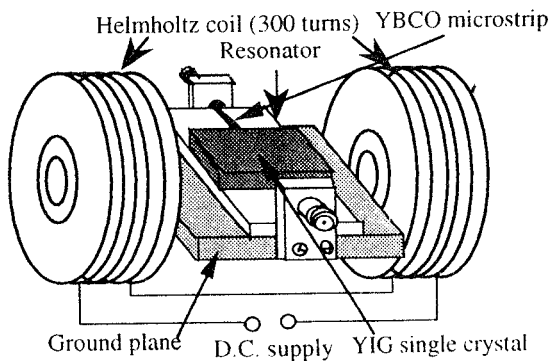


Figure 2 : Test structure with Helmholtz coil.

with the Helmholtz coil.

Experiments were conducted in the frequency range from 5.1GHz to 6.1GHz, and at the liquid nitrogen temperature of 77K. The resonator characteristics without the YIG were first examined to confirm the effect of the superconductor. The loaded quality factor  $Q_L$  of 1050 and an insertion loss of -26dB can be observed at the center frequency of 5.81GHz for the capacitive air gap of 0.5mm. This resonator quality factor is slightly lower than that of conventional superconducting resonators because the surface impedance of YBCO is about  $100 \mu \Omega$  at 4.2 K[5]. Hence the low  $Q_L$  may be due to the imperfect suppression of the radiation mode resulting from discontinuities of the terminals.

Magnetic field dependence on the superconducting resonator was confirmed experimentally. No significant changes of the center frequency or  $Q_L$  are observed for magnetic fields up to 1000 Gauss. However, for very weak magnetic fields (less than 1 Gauss), a center frequency change of about 1MHz was observed due to the vortex effect of the YBCO[3].

The characteristics of the magnetically tunable resonator were next investigated by applying the YIG single crystal. Figure 3 shows a typical frequency response of the microstrip line resonator for the capacitive air gap of 0.5mm, as a function of the dc magnetic field, up to 790 Oe. It can be seen from the figure that the center frequency  $f_0$  can be tuned magnetically from 5.24GHz to 5.42GHz, for a useful range of 200MHz.

Figure 4 shows the magnetic field dependence of  $f_0$  and  $Q_L$ . The maximum  $Q_L$  of 965 can be read from the figure, which is close to the value of the resonator without YIG. Thus no significant increase of magnetic loss at 77K was found, though such loss had been observed for the YIG film with the GGG substrate[4]. However it has a high insertion loss of 20dB. To reduce the insertion loss of the resonator, a resonator with a narrow capacitive gap ( $s=0.3$ mm) was examined. The insertion loss of the resonator at 77K was 12dB with a maximum  $Q_L$  of 762. (The  $Q_L$  of a half-

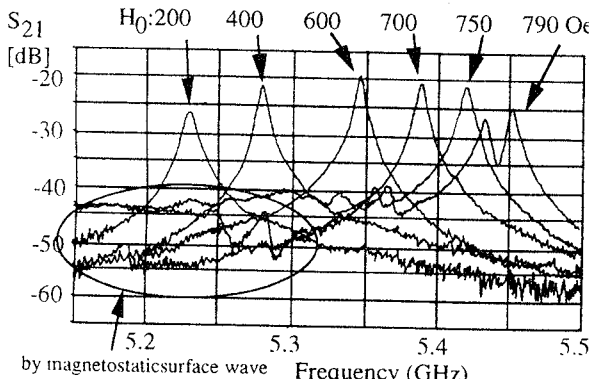


Figure 3 : Frequency response of the tunable resonator for different magnetic fields.

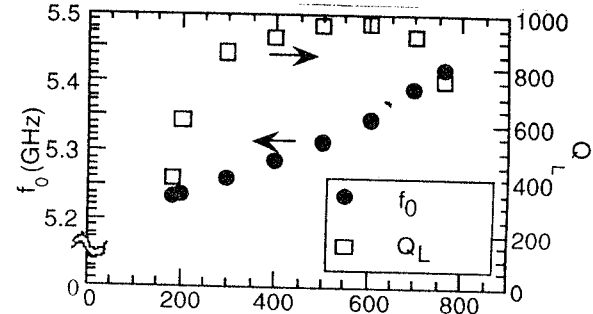


Figure 4 : Magnetic field dependence of  $f_0$  and  $Q_L$  for the resonator.

wavelength resonator using a copper microstrip line with a YIG film substrate was 166 at room temperature at 6.3GHz.)

The high sensitivity of the resonator response to the magnetic field of 200MHz of Fig.s 3 and 4 may be due to the tight coupling between the electromagnetic field on the superconducting strip through direct contact between the YIG and YBCO, and the magnetic tunability of the resonator is limited by the generation of the magnetostatic mode as discussed in the next section.

### III. DISCUSSIONS WITH DISPERSION RELATION

To compare the experimental results with theory, the dispersion relation of the microstrip line with a YIG-YBCO-MgO substrate was calculated by using the Spectrum Domain Method[6][7]. The exact analysis of the superconducting microstrip line with YIG is more complex. We assume the exact solution of the dispersion relation is derived for the TEM mode, and therefore does not include the full spectrum of the magnetostatic wave modes[7][8]. We further assume the superconducting strip is a perfect conductor. Even if these assumptions are false, the fundamental characteristics of the line will be preserved[7].

The geometry of the problem, which consists of a YIG-MgO sandwich structure, is shown in Fig. 5. The line is surrounded with an electric wall having the dimensions  $2a \times b$  to obtain the Fourier Transform.

The tensor susceptibility of the ferrite (YIG) is given by

$$\mu = \mu_0 \begin{bmatrix} 1 & 0 & 0 \\ 0 & \mu & j\kappa \\ 0 & -j\kappa & \mu \end{bmatrix} \quad (1)$$

$$\mu = 1 + \frac{\omega_h \omega_m}{\omega_h^2 - \omega^2}, \quad \kappa = \frac{\omega \omega_m}{\omega_h^2 - \omega^2}$$

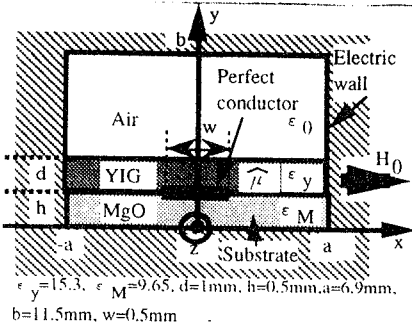


Figure 5 : Geometry of the microstrip line.

$$\omega_h = \gamma \mu_0 H_0, \quad \omega_m = \gamma \mu_0 M_0$$

$$\gamma = 1.76 \times 10^{11} \text{ rad} / (\text{T} \cdot \text{s}), \quad 4\pi M_0 = 2350 \text{ G}$$

and the dc magnetic field is applied in the x direction in Fig. 5. Helmholtz equations in the YIG region in the hybrid form, obtained from Maxwell's equation with Eq. (1), are given by

$$\frac{\partial^2}{\partial y^2} \tilde{E}_x - P \tilde{E}_x = R \tilde{H}_x, \quad \frac{\partial^2}{\partial y^2} \tilde{H}_x - Q \tilde{H}_x = S \tilde{E}_x \quad (2)$$

$$P = \beta^2 + \hat{k}_n^2 - \omega^2 \epsilon_y \mu_0 \mu_{\text{eff}}, \quad Q = j \hat{k}_n \omega \epsilon_y \frac{\kappa}{\mu}$$

$$R = \beta^2 + \frac{1}{\mu_{\text{eff}}} \hat{k}_n^2 - \omega^2 \epsilon_y \mu_0, \quad S = -j \hat{k}_n \omega \epsilon_y \frac{\kappa}{\mu}$$

The solutions of Eq. (2) after Fourier transform are given by

$$\tilde{E}_x = (A \sinh \gamma_+ y + B \cosh \gamma_+ y) + K_+ (C \sinh \gamma_- y + D \cosh \gamma_- y)$$

$$\tilde{H}_x = K_+ (A \sinh \gamma_+ y + B \cosh \gamma_+ y) + (C \sinh \gamma_- y + D \cosh \gamma_- y)$$

$$K_+ = \frac{S}{\gamma_+^2 - R}, \quad K_- = \frac{Q}{\gamma_-^2 - P}, \quad \gamma_{\pm}^2 = \frac{1}{2} (-Y \pm \sqrt{Y^2 - 4Z})$$

$$Y = -P - R, \quad Z = PR - QS$$

where  $\tilde{\cdot}$  denotes the Fourier transform.

Boundary conditions, including current distributions in the strip together with fields in the air and MgO regions, lead to an eigen value equation in the form of a Green function. The dispersion relation was derived through

$$\begin{bmatrix} K_{11}^{xx} & \cdots & K_{1J}^{xx} & | & K_{11}^{yy} & \cdots & K_{1J}^{yy} \\ \vdots & \ddots & \vdots & | & \vdots & \ddots & \vdots \\ K_{J1}^{xx} & \cdots & K_{JJ}^{xx} & | & K_{J1}^{yy} & \cdots & K_{JJ}^{yy} \\ \hline K_{11}^{yy} & \cdots & K_{1J}^{yy} & | & K_{11}^{yy} & \cdots & K_{1J}^{yy} \\ \vdots & \ddots & \vdots & | & \vdots & \ddots & \vdots \\ K_{J1}^{yy} & \cdots & K_{JJ}^{yy} & | & K_{J1}^{yy} & \cdots & K_{JJ}^{yy} \end{bmatrix} \begin{bmatrix} a_1 \\ \vdots \\ a_J \\ b_1 \\ \vdots \\ b_J \end{bmatrix} = 0 \quad (3)$$

where  $a_i, b_j$  are the unknown coefficients. Thus a nontrivial solution of the matrix  $[K]$  reduces to the dispersion relation.

Figure 6 shows the typical dispersion curve calculated numerically from Eq. (3) for an applied magnetic field of 500 Oe.

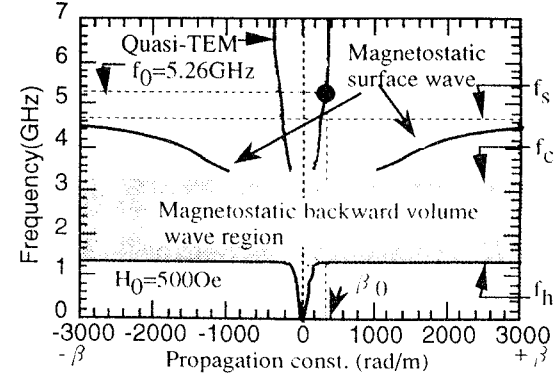


Figure 6 : Calculated dispersion curve of the line.

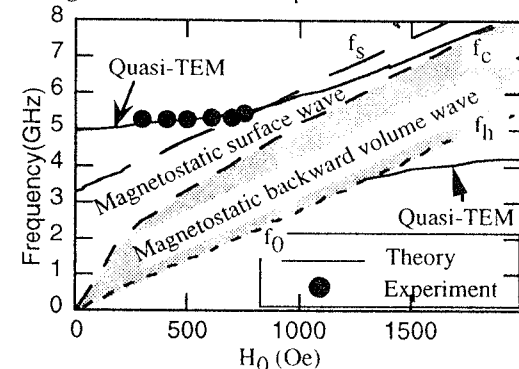


Figure 7 : Magnetostatic field dependence of dispersion curve for fixed propagation constant  $\beta_0 = \pi / 10 \text{ mm}$ .

There are two branch modes in the dispersion curve depicted in the figure. One is the TEM mode which is the main mode of the line. The other is the magnetostatic surface wave (MSSW) mode for the frequency domain between  $f_c = \gamma \mu_0 \sqrt{H_0 (H_0 + M_0)} / 2\pi$  and  $f_s = \gamma (H_0 + M_0) / 2\pi$ . The latter exhibits weak non-reciprocities, and a magnetostatic back-ward volume wave mode which radiates the wave in the dc magnetic field direction of x[7]. From another point of view, the microstrip line with YIG proposed here operates as a magnetostatic wave transducer[7][8]. However this is beyond the scope of this paper. Therefore, this dispersion curve of MSBVW between and  $f_h = \gamma H_0 / 2\pi$  and  $f_c$  is not given.

The resonance frequency  $f_0$  can be estimated by choosing point in Fig. 6; half-wavelength  $\Lambda = 10 \text{ mm} = \pi / \beta$  on the curve. The  $f_0$  of 5.26GHz at 500 Oe can be read from the figure at point  $\beta_0$  and corresponds to the experimental value of 5.31GHz at 500Oe of Fig. 4.

We can discuss the magnetic tunability of the resonator by rewriting the dispersion curve of Fig. 6 as a curve with a fixed propagation constant  $\beta_0 = \pi / \Lambda$  and changing the applied magnetic field as shown in Fig. 7. The experimental results of Fig. 4 are also plotted in Fig. 7.

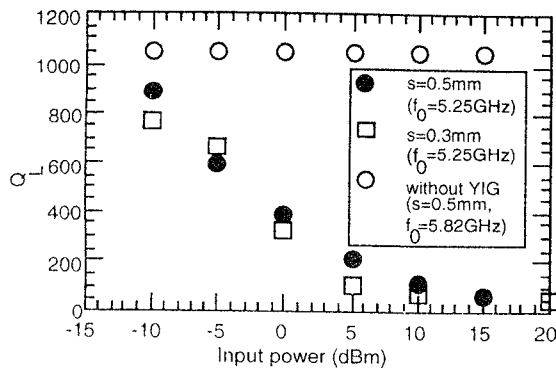


Figure 8 : Power dependence of the resonator at 77K.

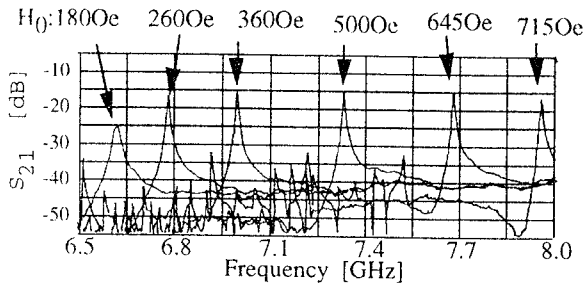


Figure 9 : Typical frequency response for the resonator magnetized longitudinal direction along the wave propagation.

From the dispersion curves of Figs. 6 and 7, it is found that the spurious responses along with resonance in the Figs. 3 are the frequency responses of the MSSW mode[8]. This mode will degrade the resonator response in the configuration discussed here. Thus experimental results agree well with theory.

In the experiments, the effect of the YIG on  $Q_L$  with magnetic loss  $\Delta H$  was not found at 77K. This may be a negligible effect on the temperature dependence of the magnetic line width

$\Delta H$  for the pure YIG crystal. However, to develop resonance characteristics, the YIG slab should be less than 1mm thick considering the reduction of radiation loss due to the discontinuity of the strip line.

We measured the power dependence of the resonator with YIG at 77K as shown in Fig. 8 for different air gaps  $s$  in the strip line resonator of Fig. 1. It can be seen from the figure that the resonator input power significant by reduces  $Q_L$ . The saturation level is -10dBm, which is a considerably lower power level than for the case without YIG[5] as shown in the figure by open circles. This may be attributed to the nonlinear effect of the YIG single crystal.

Finally, we have examined by changing the bias magnetic field direction from transverse to longitudinal *i.e.* along the wave propagation, wide band magnetically tunable characteristic of more than 1.5GHz has been observed and is shown in Fig. 9.

#### IV. CONCLUSION

Magnetically tunable superconducting single resonators

using YIG single crystal have been demonstrated. A tunability of 200MHz with maximum  $Q_L$  of 965 has been achieved for a half-wavelength microstrip line in which a YIG single crystal is put onto the superconducting strip. The dispersion relation for the experimental result was discussed briefly with the theory on mixed solutions of TEM and MSW modes and agreed well with the predicted value.

To develop the resonator characteristics further, the discontinuity problems between YIG and the microstrip line should be investigated, and temperature dependence of the magnetic loss of the YIG should be also studied. As a result, a superconducting filter using a YIG single crystal was developed and exhibited better magnetic tunable characteristics than the YIG film and may be useful for the microwave receiver front end with a small tuning coil.

#### V. ACKNOWLEDGEMENT

This work was supported partly by NEC corporation. We would like to thank Dr. T. Inui and Dr. T. Yoshitake for fabricating the superconducting resonator.

#### References

- [1] E. Denlinger, R. Paglione, D. Kalokitis, E. Belohoubek, A. Pique, X. D. Wu, T. Venkatesan, A. Fathy, V. Pendrik S. Green, and S. Matheuis, "Superconducting Nonreciprocal Devices for Microwave Systems," *IEEE Microwave and Guided Wave Letts.*, vol.2, pp.449-451, Nov. 1992.
- [2] G. F. Dionne, D. E. Oates, D. H. Temme, and J. A. Weiss, "Ferrite-Superconductor Devices for Advanced Microwave Applications," *IEEE Trans. Microwave Theory Tech.*, vol.44, no.7, pp.1361-1368, July 1996.
- [3] A. Trotel, M. Pyee, B. Lavigne, D. Chambonnet, and P. Ledere, "Magnetically tunable YBaCuO microstrip resonators and bandpass filters," *Appl. Phys. Lett.* 68, (18), 29, pp.2559-2561, Apr. 1996.
- [4] M. Tsutsumi, T. Fukusako, and H. Shimasaki, "Magnetically tunable superconductor filters using yttrium iron garnet films," *IEEE Trans. on Magnetics*, vol.31, no.6, pp.3467-3469, Nov. 1995.
- [5] T. Yoshitake, H. Tsuge, and T. Inui, "Effect of microstructure of  $YBa_2Cu_3O_x$  films on power handling capability studied with microstrip resonators," *J.Appl.Phys.*, vol.76, NO.7, 1, pp.4256-4261, Oct. 1994.
- [6] M. Tsutsumi, and T. Asahara, "Microstrip lines using yttrium iron garnet Film," *IEEE Trans. Microwave Theory Tech.*, vol.38, pp.1461-1467, Oct. 1990.
- [7] T. Fukusako, and M. Tsutsumi, "Microstrip line using yttrium iron garnet," *Technical report of IEICE*, SAT-52, MW96-63, pp.75-80, July 1996.
- [8] D. D. Stancil, "Theory of Magnetostatic Waves," *Springer-Verlag*, 1993.